Interference Analysis and Transmit Power Control in IEEE 802.11a/h Wireless LANs

Daji Qiao, *Member, IEEE*, Sunghyun Choi, *Senior Member, IEEE*, and Kang G. Shin, *Fellow, IEEE*

***Abstract*—Reducing the energy consumption by wireless communication devices is perhaps the most important issue in the widely deployed and dramatically growing IEEE 802.11 WLANs (wireless local area networks). TPC (transmit power control) has been recognized as one of the effective ways to achieve this goal. In this paper, we study the emerging 802.11a/h systems that provide a structured means to support intelligent TPC. Based on a rigorous analysis of the relationship among different radio ranges and TPC's effects on the interference, we present an optimal low-energy transmission strategy, called *MiSer*, which is deployed in the format of *RTS-CTS(strong)-Data(MiSer)-Ack*. The key idea of MiSer is to combine TPC with PHY (physical layer) rate adaptation and compute offline an optimal rate–power combination table, then at runtime, a wireless station determines the most energy-efficient transmission strategy for *each* data frame transmission by a simple table lookup. Simulation results show MiSer's clear superiority to other two-way or four-way frame exchange mechanisms in terms of energy conservation.**

***Index Terms*—IEEE 802.11a/h, interference analysis, MiSer, PHY rate adaptation, TPC, transmit power control.**

I. Introduction

MOST wireless stations, such as laptops and palmtops, are battery-powered and hence must operate with a limited amount of energy. It is, therefore, very important to reduce the energy consumption by wireless communication devices. In this paper, we study the energy conservation issue in the IEEE 802.11 WLANs (wireless local area networks), or more specifically, the emerging 802.11a/h systems.

A WLAN device can be in one of the following modes: *transmit mode*, *receive mode*, *idle mode*, or *doze mode*. It consumes the highest power in the transmit mode and very little energy in the doze mode. In the idle mode, a WLAN device is required to sense the medium, and hence, consumes a similar amount of power as when it is in the receive mode [1]. Several power-management policies [1]–[5] have been proposed to force a WLAN device to enter the doze mode adaptively at appropriate moments to save battery energy.

Manuscript received November 24, 2003; revised March 21, 2005, and December 5, 2005; approved by IEEE/ACM TRANSACTIONS ON NETWORKING Editor N. Shroff. This work was supported in part by the Air Force Office of Scientific Research (AFOSR) under Grants F49620-00-1-0327 and F49620-01-1-0120.

D. Qiao is with the Department of Electrical and Computer Engineering, Iowa State University, Ames, IA 50011 USA (e-mail: daji@iastate.edu).

S. Choi is with the School of Electrical Engineering, Seoul National University, Kwanak, Seoul 151-600, Korea (e-mail: schoi@snu.ac.kr).

K. G. Shin is with the Department of Electrical Engineering and Computer Science, University of Michigan, Ann Arbor, MI 48109-2122 USA (e-mail: kgshin@umich.edu).

Digital Object Identifier 10.1109/TNET.2007.900381

An alternative way to conserve energy is to apply TPC (transmit power control) in WLAN systems [6]–[9], which allows a WLAN device to use the minimum required power level in the transmit mode and is complementary to the power-management policies. In this paper, we first provide a thorough analysis of the interference in 802.11a systems, then present a novel intelligent TPC mechanism, called *MiSer* [10], to minimize the communication energy consumption.

A. Motivation and Key Contributions

IEEE 802.11 [11] specifies two different MAC (medium access control) schemes in WLANs: the contention-based DCF (distributed coordination function) and the polling-based PCF (point coordination function). At present, most 802.11-compliant products only implement the mandatory DCF. Thus, we only consider the DCF in this paper.

Among the IEEE 802.11 PHYs (physical layers) [12]–[14], the 802.11a PHY [14] has received significant attention because it supports a wider range of transmission rates (eight rates from 6 to 54 Mb/s) and operates at the cleaner 5-GHz frequency band. Moreover, the 802.11h standard [15], which is an extension to the 802.11 MAC and the 802.11a PHY, provides a transmit-power reporting mechanism that makes intelligent TPC feasible at the MAC layer. So, it is important to have a well-designed TPC mechanism work with the 802.11a/h such that its TPC capability and multiple transmission rates can be fully exploited.

Note that, due to the contention nature of the DCF, the effectiveness of a TPC mechanism hinges on the condition that application of TPC on data transmissions will not aggravate the "hidden nodes" problem or the interference in the network [16]. A natural way to deal with this problem is to exchange RTS/CTS frames to reserve the wireless channel prior to each data transmission attempt, which has been used in many proposed TPC mechanisms [6]–[8], [17], [18]. Our preliminary study in [19] considered the simple infrastructure DCF system where hidden nodes are completely eliminated with RTS/CTS support. This problem becomes more complicated in an ad hoc DCF system[1] where the wireless stations, if within each other's communication range, communicate directly. Since not every wireless station may be able to hear directly from all other stations, the RTS/CTS mechanism cannot guarantee elimination of the hidden nodes. Moreover, applying TPC on data transmissions, even with RTS/CTS support, aggravates the interference in an ad hoc DCF system.

[1]The term *ad hoc* in the context of ad hoc DCF systems [11] refers to IBSS (independent basic service set), which emphasizes no infrastructure support from the AP (access point); the wireless stations, if within each other's communication range, communicate directly (i.e., single-hop transmissions). It is different from the term *ad hoc* in the context of mobile ad hoc networks, which emphasizes multi-hop transmissions.

The first contribution of this paper is to provide a rigorous analysis of the relationship among different radio ranges and TPC's effects on the interference in 802.11 systems. Then, based on the interference analysis, we propose application of TPC in 802.11a systems in the following way: in addition to exchanging RTS/CTS frames before each data transmission attempt, the CTS frames are transmitted at a stronger power level to ameliorate the TPC-caused interference.

The second contribution of this paper is the development of a novel *per-frame-based* intelligent TPC mechanism for 802.11a/h systems, called *MiSer* (Minimum-energy transmission Strategy) [10], under the assumption that wireless channel models are available. MiSer is deployed in the format of *RTS-CTS(strong)-Data(MiSer)-Ack* and can be used in both infrastructure and ad hoc DCF systems. Obviously, the lower the transmit power or the higher the PHY rate (hence, the smaller the transmission time), the less energy consumed in one single transmission attempt, but more likely the transmission will fail, thus causing retransmissions and eventually consuming more energy. So, there are inherent tradeoffs, and the key idea of MiSer is to combine TPC with PHY rate adaptation and pre-establish a rate–power combination table indexed by the *data transmission status* quintuplet that consists of the data payload length, the path loss, the receiver-side wireless channel condition, and two frame retry counts. Each entry of the table is the optimal rate–power combination that maximizes the energy efficiency—which is defined as the ratio of the expected delivered data payload to the expected total energy consumption—under the corresponding data transmission status. At runtime, a wireless station determines the best transmit power as well as the proper PHY rate for each data transmission attempt by a simple table lookup, using the most up-to-date data transmission status as the index.

B. Related Work

Various TPC schemes have been proposed [6]–[9] to conserve energy in wireless networks. One common problem of these schemes is that none of them considered PHY rate adaptation—a key component of MiSer. Since the 802.11 PHYs support multiple transmission rates, utilizing them adaptively by choosing the best PHY rate at a given time can enhance the system performance significantly. In fact, our simulation results in Section V show that PHY rate adaptation is very effective in saving energy. Hence, PHY rate adaptation should be considered in conjunction with TPC.

In [17] and [18], the authors proposed an adaptive transmission protocol for spread-spectrum networks, which adjusts the power in a transmitted data frame and the rate of the Reed–Solomon (RS) code to respond to variations in the propagation loss and partial-band interference. Instead of finding the optimal combination of power and code rate for each data transmission, the proposed protocol adopts a two-step approach by determining the code rate first and then the power, hence, is sub-optimal. Although the authors used RTS/CTS frame exchanges to deal with the "hidden nodes" problem in the proposed protocol, they overlooked the fact that applying TPC on data transmissions aggravates the interference, even in a wireless network with RTS/CTS support, and may result in serious system performance degradation.

The authors of [20] and [21] proposed a lazy scheduling algorithm and an iterative MoveRight algorithm, respectively, to minimize the energy used to transmit packets from a wireless station to a single receiver or to multiple receivers. The key idea is to transmit packets for a long period with lower transmit power as long as the deadline constraint is met. However, they assumed that the wireless channel is time-invariant and focused on devising optimal schedules for a wireless station to transmit multiple packets (sharing the same deadline constraint), which is different from the issues we address in this paper.

C. Organization

The rest of this paper is organized as follows. For completeness, Section II briefly introduces the DCF of the IEEE 802.11 MAC and the IEEE 802.11a PHY. In Section III, following a theoretical analysis of the relationship among different radio ranges and TPC's effects on the interference in 802.11a systems, an enhanced RTS-CTS(strong)-Data(TPC)-Ack mechanism is proposed and justified to accommodate intelligent TPC. Section IV describes the details of MiSer and discusses the related implementation issues. Section V presents and evaluates the simulation results, and finally, the paper concludes in Section VI.

II. System Overview

A. DCF of the 802.11 MAC

The DCF [11], as the basic access scheme of the 802.11 MAC, achieves automatic medium sharing among compatible stations via the use of CSMA/CA (carrier-sense multiple access with collision avoidance). A wireless station is allowed to transmit only if its carrier-sense mechanism determines that the medium has been idle for at least DIFS (distributed inter-frame space) time. Moreover, in order to reduce the collision probability among multiple stations accessing the medium, a station is required to select a random backoff interval after deferral, or prior to attempting to transmit another frame after a successful transmission.

The SIFS (short inter-frame space), which is smaller than the DIFS, is the time interval used between transmissions within a frame exchange sequence, e.g., a two-way Data-Ack handshake or a four-way RTS-CTS-Data-Ack handshake. Using this small gap prevents other stations—which are required to wait for the medium to be idle for a longer gap (i.e., at least DIFS time)—from attempting to use the medium, thus giving priority to completion of the in-progress frame exchange. On the other hand, if a CTS (Ack) frame is not received, the transmitter will contend again for the medium to retransmit the frame after a CTS (Ack) timeout.

The DCF includes a virtual sensing mechanism, called the NAV (network allocation vector), in addition to physical sensing. The NAV is a value that indicates to a station the remaining time before the wireless medium becomes available, and it is updated upon each RTS/CTS frame reception using the Duration/ID value carried in the frame header. By examining the NAV, a station avoids transmitting a frame that may interfere with the subsequent Data/Ack frame exchange even when the wireless medium appears to be idle according to physical sensing.

The 802.11 MAC requires that a wireless station maintain a short retry count (SRC) and a long retry count (LRC) for each data frame, and these counts are incremented and reset independently. When the RTS-CTS-Data-Ack handshake is used to transmit a data frame, SRC (LRC) is incremented every time an RTS (Data) transmission fails. The data frame is discarded when either SRC reaches *dot11ShortRetryLimit* or LRC reaches *dot11LongRetryLimit*. The default values of *dot11ShortRetryLimit* and *dot11LongRetryLimit* are 7 and 4, respectively. Note that both SRC and LRC are reset to 0 *only* after a successful data transmission or after a data frame is discarded.

B. The 802.11a PHY

The 802.11a PHY [14] is based on orthogonal frequency division multiplexing (OFDM) and provides eight PHY rates (from 6 to 54 Mb/s) by employing different modulation schemes and convolutional codes at the 5 GHz U-NII (Unlicensed National Information Infrastructure) band. The frame exchange between MAC and PHY is under the control of the PLCP (physical layer convergence procedure) sublayer.

III. Interference Analysis in 802.11 Systems

Applying TPC, which allows a WLAN device to use the minimum required power level in the transmit mode, is naturally an attractive way to save battery energy. However, due to the contention nature of the DCF, the effectiveness of a TPC mechanism hinges on the condition that application of TPC on data transmissions will not aggravate the "hidden nodes" problem or the interference in the network. In this section, we first investigate the relationship among different radio ranges and TPC's effects on the interference in 802.11 systems, then propose a novel way to apply TPC in 802.11a systems while ameliorating the TPC-caused interference, and justify it based on a theoretical analysis.

A. Radio Ranges in 802.11 Systems

In general, there are four different radio ranges in an 802.11 system: *transmission range*, *NAV set range*, *CCA busy range*, and *interference range*.

- *Transmission range* is central to the transmitter and represents the range within which the receiver station can receive a frame successfully, assuming no interference from neighboring stations. It varies with the data payload length, the PHY rate, the transmit power, the radio propagation property that determines the path loss, and the receiver-side wireless channel condition.
- *NAV set range* is the range within which neighboring stations can set the NAVs correctly based on the Duration/ID information carried in the RTS/CTS frames and will not interfere with the subsequent Data/Ack frame exchange. Since RTS/CTS frames are always transmitted at a fixed rate (e.g., 6 Mb/s in 802.11a systems), the NAV set range is independent of the data rate.
- *CCA busy range* is central to the transmitter and represents the range within which neighboring stations can physically sense the channel busy during the data transmission (by the transmitter) and then defer their own transmission attempts. There are two methods for a wireless station to report CCA (clear channel assessment) busy. One is based on *carrier detection*, and the other is based on *energy detection* by which a wireless station will report a busy medium upon detection of any signal power above the ED (Energy Detection) threshold.
- *Interference range* is central to the receiver and represents the range within which neighboring stations are able to interfere with the reception of data frames at the receiver.

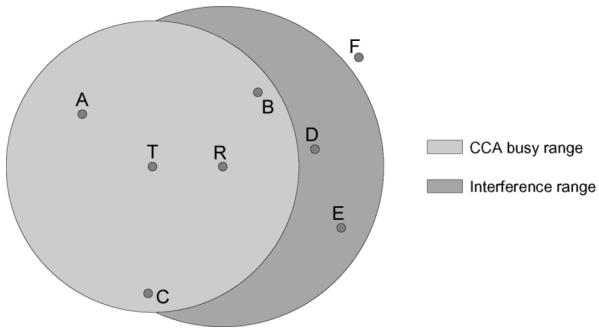

Fig. 1. Sketch of the radio ranges during a two-way handshake.

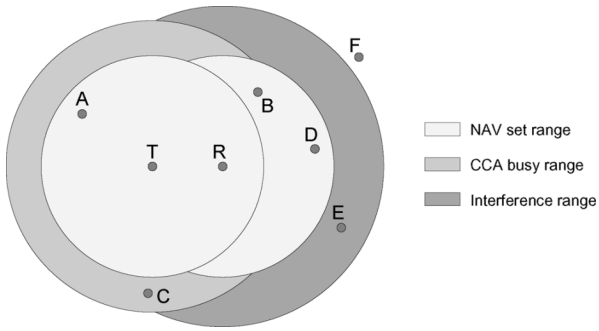

Fig. 2. Sketch of the radio ranges during a four-way handshake.

B. TPC's Effects on the Interference in 802.11 Systems

Figs. 1 and 2 sketch the relative positions of different radio ranges when the transmitter (T) transmits a data frame to the receiver (R) using the two-way Data-Ack handshake and the four-way RTS-CTS-Data-Ack handshake, respectively. NAV set range, CCA busy range, and interference range are shown as the light-, medium-, and dark-shaded areas, respectively. The NAV set range is actually the conjunction of the RTS transmission range and the CTS transmission range. Note that the sizes of radio ranges vary with 802.11 systems equipped with different PHYs.

A, B, C, D, E, and F are the six neighboring stations. As shown in Fig. 1, when the two-way handshake is used, A, B, C, and F will not interfere with the Data/Ack frame exchange. This is because A, B, and C can physically sense the channel busy, while F is outside the interference range. On the other hand, D and E are unable to sense the data transmission, but are close enough to the receiver (within the interference range) to cause the interference. They are often referred to as the "hidden nodes" to T. In order to alleviate such "hidden nodes" problem, T and R may exchange RTS/CTS frames to reserve the wireless channel before the actual data transmissions, as shown in Fig. 2. This

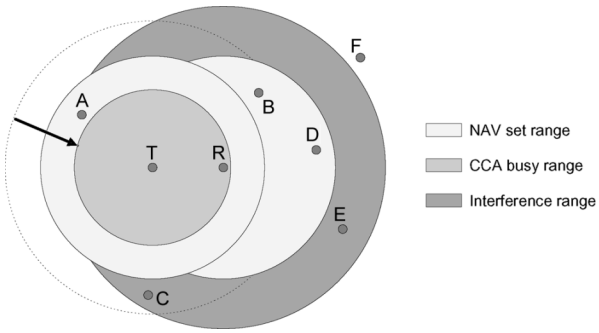

Fig. 3. Aggravated interference caused by the shrunk CCA busy range.

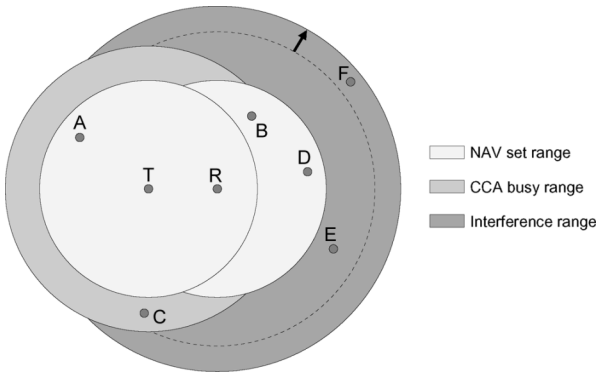

Fig. 4. Aggravated interference caused by the enlarged interference range.

way, D sets its NAV upon CTS reception and will not interfere with the subsequent Data/Ack frame exchange.

Now, let us see how the radio ranges are affected when TPC is applied on data transmissions. Since the kernel idea of TPC is to transmit a data frame at the minimum required power level, so when the two-way handshake is used, it may result in more hidden nodes in the network. For example, B becomes a hidden node to T when TPC is applied with the two-way handshake (see Fig. 1), while it will not interfere with the Data/Ack frame exchange when the four-way handshake is used as it is covered by the NAV set range (see Fig. 2). In fact, even with RTS/CTS support, applying TPC on data transmissions may still aggravate the interference in the following ways.

- *Scenario I*: The interference may be aggravated due to shrinkage of the CCA busy range. For example, comparing Fig. 3 with Fig. 2, we can see that, station C originally deferred its transmission attempt based on physical sensing but is now outside the shrunk CCA busy range, and hence may interfere with the Data/Ack frame exchange. Note that, however, this scenario may occur *only* when the original CCA busy range is larger than the NAV set range.
- *Scenario II*: The interference may be aggravated due to enlargement of the interference range. For example, comparing Fig. 4 with Fig. 2, we can see that, station F was originally outside the interference range but is now within the enlarged interference range, and hence may interfere with the data frame reception.

The above aggravated interference scenarios, as results of applying TPC on data transmissions, indicate the importance of ameliorating the TPC-caused interference to the effectiveness of an intelligent TPC mechanism.

C. NAV Set Range Versus CCA Busy Range in 802.11a Systems

According to the 802.11a standard [14], the *receiver minimum input level sensitivity* is defined as the received signal strength level at which the packet error rate (PER) of a 1000-octet frame is less than 10%. It is rate-dependent and different sensitivity levels for different PHY rates are listed in [14, Table 91]. For example, the receiver minimum sensitivity level for 6 Mb/s is -82 dBm. Since the length of an RTS/CTS frame is much shorter than 1000 octets and they are transmitted at the most robust 6 Mb/s, the PER of an RTS/CTS frame at the minimum 6-Mb/s sensitivity level (-82 dBm) is almost zero. Therefore, it is safe to say that the RTS/CTS transmission range in an 802.11a system corresponds to the minimum 6-Mb/s sensitivity level (-82 dBm). Recall that the NAV set range is the conjunction of the RTS transmission range and the CTS transmission range.

On the other hand, the *CCA sensitivity* is defined (in [14, Clause 17.3.10.5]) as: "The start of a valid OFDM transmission at a receive level equal to or greater than the minimum 6-Mb/s sensitivity (-82 dBm) shall cause CCA to indicate busy with a probability $>90\%$ within 4 μs. If the preamble portion was missed, the receiver shall hold the carrier sense (CS) signal busy for any signal 20 dB above the minimum 6-Mb/s sensitivity." Therefore, the CCA busy sensitivity levels based on carrier detection and energy detection are -82 dBm and -62 dBm, respectively, regardless of the data transmission rate.

We can make the following important observation: *when the four-way handshake is used in an 802.11a system to transmit a data frame, the CCA busy range is completely covered by the NAV set range*. This unique feature of 802.11a systems is due to the fact that, the 802.11a PHY's ED threshold is set 20 dB higher than the carrier detection threshold, which is different from other 802.11 PHYs such as the 802.11b. As a result, *Scenario I* described in Section III-B will never occur in an 802.11a system, while it may cause serious interference in 802.11b systems. On the other hand, the enlargement of the interference range aggravates the interference in both 802.11a and 802.11b systems.

D. NAV Set Range Versus Interference Range in 802.11a Systems

Since the signal power needed for interrupting a frame reception is much lower than that of delivering a frame successfully [22], under certain circumstances—especially, when TPC is used for data transmissions, as will be shown below—the interference range may be larger than the NAV set range. We now investigate the relationship between the transmit power and the interference range when four different four-way handshakes are used in an 802.11a system.

1) RTS-CTS-Data-Ack: At first, let us consider the conventional four-way handshake, where all frames are transmitted at the same nominal power level ($\mathcal{P}_{nom}$).[2] As shown in Fig. 5, the distance between T and R is d. Let $d_{tx\_rc,6mbps}$ denote the radius of the RTS/CTS transmission range. So, we have

$$r_t = r_r = d_{tx\_rc,6mbps} \geqslant d. \tag{1}$$

[2]In the following analysis, we let $\mathcal{P}_{nom}$ be 15 dBm, the nominal transmit power of Netgear WAG511 802.11a/b/g Dual Band Wireless PC Cards [23].

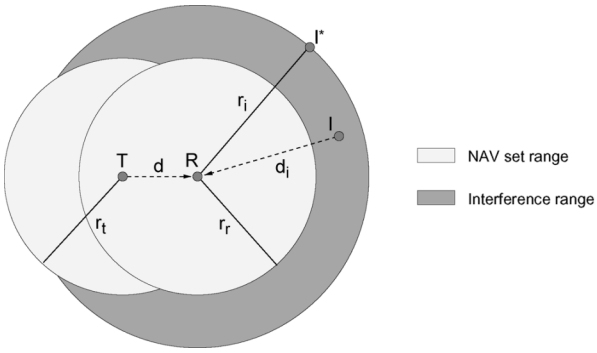

Fig. 5. NAV set range versus interference range.

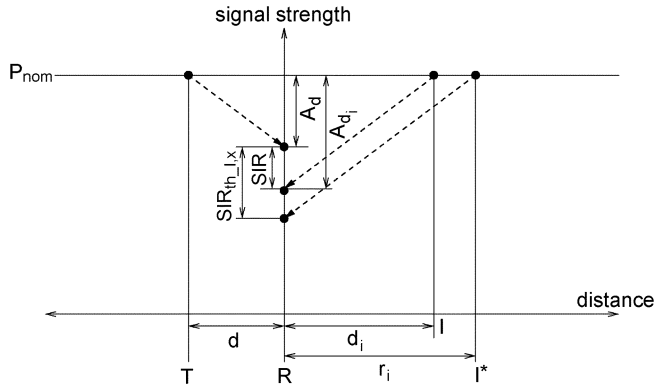

Fig. 6. Without TPC, the size of the interference range varies with the data payload length, the transmission rate, and the distance between the transmitter and the receiver.

Note that the CCA busy range is not shown in Fig. 5, as it is completely covered by the NAV set range in 802.11a systems and has no effects on the following analysis.

Fig. 6 illustrates the radius of the interference range (r_i) when T transmits (at rate x) a data frame (with payload ℓ) to R. Let $\mathrm{SIR}_{th\_\ell,x}$ be the signal-to-interference ratio (SIR) threshold above which the data frame can be received successfully. Therefore, a neighboring station I interferes with the data frame reception if the following condition holds:

$$\begin{aligned}\mathrm{SIR}_{th\_\ell,x} \geqslant \mathrm{SIR} &= \mathcal{P}_{r,data} - \mathcal{P}_{r,int} \\ &= (\mathcal{P}_{t,data} - \mathcal{A}_d) - (\mathcal{P}_{t,int} - \mathcal{A}_{d_i}) \\ &= (\mathcal{P}_{nom} - \mathcal{A}_d) - (\mathcal{P}_{nom} - \mathcal{A}_{d_i}) \\ &= \mathcal{A}_{d_i} - \mathcal{A}_d = \left(\frac{d_i}{d}\right)^4 \qquad (2)\end{aligned}$$

$$\iff \quad d_i \leqslant \sqrt[4]{\mathrm{SIR}_{th\_\ell,x}} \cdot d. \qquad (3)$$

$\mathcal{P}_{t,data}$, $\mathcal{P}_{r,data}$, $\mathcal{P}_{t,int}$, and $\mathcal{P}_{r,int}$ are the transmit power of the data frame, the received data signal strength, the transmit power of the interference signal, and the received interference signal strength (all in dBm), respectively. $\mathcal{A}_d$ and $\mathcal{A}_{d_i}$ are the path losses (in dB) over distances d and d_i, respectively. Eq. (2) is obtained by assuming the log-distance path loss model with path loss exponent of four [24], which is suitable for indoor office environments. Eq. (3) implies that the radius of the interference range is

$$r_i = \sqrt[4]{\mathrm{SIR}_{th\_\ell,x}} \cdot d. \qquad (4)$$

We have two observations. First, when the conventional four-way handshake is used, the size of the interference range varies with the data payload length (ℓ), the transmission rate (x), and the distance (d) between the transmitter and the receiver. Only when d is larger than a certain value, the NAV set range will not be able to cover the interference range, i.e.,

$$d > \frac{d_{tx\_rc,6mbps}}{\sqrt[4]{\mathrm{SIR}_{th\_\ell,x}}} \quad \Longrightarrow \quad r_i > r_r \qquad (5)$$

and then the neighboring stations that are inside the interference range but outside the NAV set range can interfere with the data frame reception. Second, the interference signal could be RTS, CTS, Data, or Ack frames.

2) RTS-CTS-Data(TPC)-Ack: Now, let us examine how the interference range is affected when we only apply TPC on data transmissions while keeping the transmit power of RTS, CTS, and Ack frames at the nominal level. Consider the same configuration as shown in Fig. 5.

With TPC, as illustrated in Fig. 7, the transmitter adapts its transmit power in such a way that the received data signal strength is always kept at the minimum required level, i.e.,

$$\mathcal{P}_{t,data} \leqslant \mathcal{P}_{nom} \qquad (6)$$

and

$$\mathcal{P}_{t,data} - \mathcal{A}_d = \mathcal{P}_{nom} - \mathcal{A}_{d_{tx\_\ell,x}} \qquad (7)$$

where $d_{tx\_\ell,x}$ is the transmission range when a data frame with payload ℓ is transmitted at rate x using the nominal transmit power. Therefore, the condition for an interference to occur becomes

$$\begin{aligned}\mathrm{SIR}_{th\_\ell,x} \geqslant \mathrm{SIR} &= \mathcal{P}_{r,data} - \mathcal{P}_{r,int} \\ &= (\mathcal{P}_{t,data} - \mathcal{A}_d) - (\mathcal{P}_{t,int} - \mathcal{A}_{d_i}) \\ &= \left(\mathcal{P}_{nom} - \mathcal{A}_{d_{tx\_\ell,x}}\right) - (\mathcal{P}_{t,int} - \mathcal{A}_{d_i}) \\ &\geqslant \left(\mathcal{P}_{nom} - \mathcal{A}_{d_{tx\_\ell,x}}\right) - (\mathcal{P}_{nom} - \mathcal{A}_{d_i}) \\ &= \mathcal{A}_{d_i} - \mathcal{A}_{d_{tx\_\ell,x}}. \qquad (8)\end{aligned}$$

On the other hand, when the data frame carries a larger payload $(\ell' > \ell)$ or is transmitted at a higher rate $(x' > x)$, a higher receiver-side SIR is required to have a successful frame reception $(\mathrm{SIR}_{th\_\ell',x'} > \mathrm{SIR}_{th\_\ell,x})$, and consequently, the transmission range shrinks $(d_{tx\_\ell',x'} < d_{tx\_\ell,x})$. Recall that the transmission range represents the maximum distance over which the receiver can receive a data frame successfully. Hence, as shown in Fig. 8, the received data signal strength on the edge of the transmission range is always at the minimum required level:

$$\begin{aligned}&\mathcal{P}_{nom} - \left(\mathcal{A}_{d_{tx\_\ell,x}} + \mathrm{SIR}_{th\_\ell,x}\right) \\ &\quad = \mathcal{P}_{nom} - \left(\mathcal{A}_{d_{tx\_\ell',x'}} + \mathrm{SIR}_{th\_\ell',x'}\right) \\ &\iff \mathcal{A}_{d_{tx\_\ell,x}} + \mathrm{SIR}_{th\_\ell,x} = \mathcal{A}_{d_{tx\_\ell',x'}} + \mathrm{SIR}_{th\_\ell',x'}. \qquad (9)\end{aligned}$$

Therefore, (8) is equivalent to

$$\begin{aligned}&\mathrm{SIR}_{th\_rc,6mbps} \geqslant \mathcal{A}_{d_i} - \mathcal{A}_{d_{tx\_rc,6mbps}} \\ &\iff \mathrm{SIR}_{th\_rc,6mbps} \geqslant \left(\frac{d_i}{d_{tx\_rc,6mbps}}\right)^4 \\ &\iff d_i \leqslant \sqrt[4]{\mathrm{SIR}_{th\_rc,6mbps}} \cdot d_{tx\_rc,6mbps}. \qquad (10)\end{aligned}$$

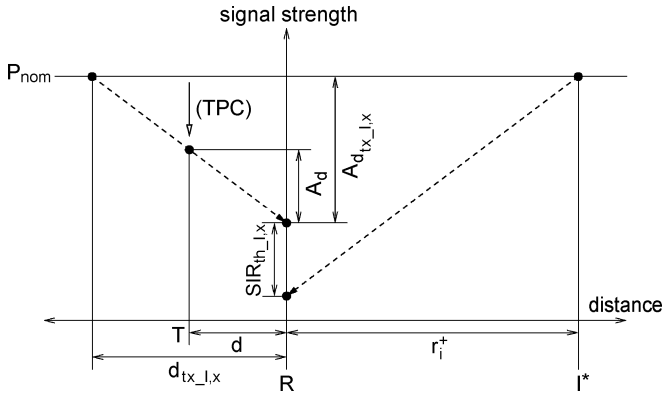

Fig. 7. With TPC, the size of the interference range is independent of the distance between the transmitter and the receiver.

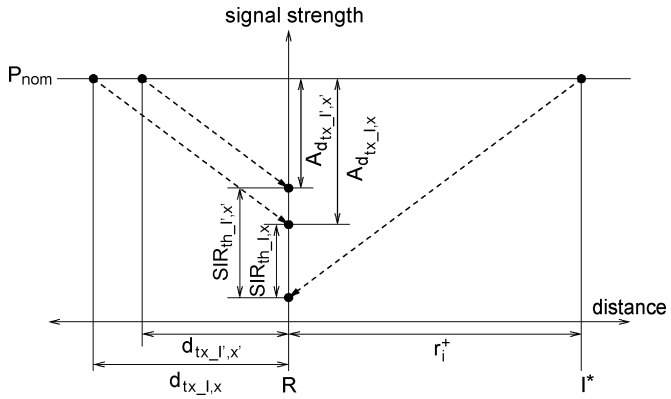

Fig. 8. With TPC, the size of the interference range is also independent of the data payload length and the transmission rate.

The radius of the interference range becomes

$$r_i^+ = \sqrt[4]{\mathrm{SIR}_{th\_rc,6mbps}} \cdot d_{tx\_rc,6mbps}. \tag{11}$$

It is interesting to see that the size of the interference range is now independent of the data payload length (ℓ), the transmission rate (x), and the distance (d) between the transmitter and the receiver, unlike when the conventional four-way handshake is used. Moreover, since $\mathrm{SIR}_{th\_rc,6mbps} > 1$, we have

$$r_i^+ > d_{tx\_rc,6mbps} = r_r \tag{12}$$

which means that the interference range is always larger than the NAV set range. As a result, there are always potential hidden nodes to interfere with the data frame reception, meaning that the interference is aggravated. This is actually the *Scenario II* described in Section III-B. The interference signal could be RTS, CTS, Data, or Ack frames.

3) RTS-CTS(Strong)-Data(TPC)-Ack: One way to deal with the aggravated interference problem caused by TPC is to transmit the CTS frames at a stronger power level ($\mathcal{P}_{cts^+} = \alpha \cdot \mathcal{P}_{nom}$ with $\alpha > 1$). The NAV set range is now enlarged to

$$\begin{cases} r_t = d_{tx\_rc,6mbps} \\ r_r^+ = \sqrt[4]{\alpha} \cdot r_r = \sqrt[4]{\alpha} \cdot d_{tx\_rc,6mbps}. \end{cases} \tag{13}$$

Consider the same configuration as shown in Fig. 5. When the interference signal is an RTS, Data, or Ack frame, since these frames are transmitted at or lower than the nominal power level, the analysis in Section III-D2 holds and we have

$$r_i^+ = \sqrt[4]{\mathrm{SIR}_{th\_rc,6mbps}} \cdot d_{tx\_rc,6mbps}. \tag{14}$$

Comparing (13) with (14), we can see that, when

$$\alpha \geqslant \mathrm{SIR}_{th\_rc,6mbps} \tag{15}$$

the enlarged NAV set range covers the interference range completely, i.e.,

$$\begin{aligned} &\alpha \geqslant \mathrm{SIR}_{th\_rc,6mbps} \\ \Longleftrightarrow\ &\sqrt[4]{\alpha} \cdot d_{tx\_rc,6mbps} \geqslant \sqrt[4]{\mathrm{SIR}_{th\_rc,6mbps}} \cdot d_{tx\_rc,6mbps} \\ \Longleftrightarrow\ &r_r^+ \geqslant r_i^+ \end{aligned}$$

and hence, the data frame reception will never be interfered with by any RTS, Data, or Ack frames from neighboring stations.

On the other hand, when the interference signal is a stronger-power-transmitted CTS frame, the condition for an interference to occur becomes

$$\begin{aligned} \mathrm{SIR}_{th\_\ell,x} \geqslant \mathrm{SIR} &= \mathcal{P}_{r,data} - \mathcal{P}_{r,int(cts^+)} \\ &= (\mathcal{P}_{t,data} - \mathcal{A}_d) - (\mathcal{P}_{t,int(cts^+)} - \mathcal{A}_{d_i}) \\ &= (\mathcal{P}_{nom} - \mathcal{A}_{d_{tx\_\ell,x}}) - (\mathcal{P}_{cts^+} - \mathcal{A}_{d_i}) \\ &= \mathcal{A}_{d_i} - \mathcal{A}_{d_{tx\_\ell,x}} - (\mathcal{P}_{cts^+} - \mathcal{P}_{nom}). \end{aligned} \tag{16}$$

Following a similar argument as in Section III-D2, (16) is equivalent to

$$\begin{aligned} &\mathrm{SIR}_{th\_rc,6mbps} \geqslant \mathcal{A}_{d_i} - \mathcal{A}_{d_{tx\_rc,6mbps}} - (\mathcal{P}_{cts^+} - \mathcal{P}_{nom}) \\ \Longleftrightarrow\ &\mathrm{SIR}_{th\_rc,6mbps} \geqslant \left(\frac{d_i}{d_{tx\_rc,6mbps}}\right)^4 \cdot \frac{1}{\alpha} \\ \Longleftrightarrow\ &d_i \leqslant \sqrt[4]{\alpha \cdot \mathrm{SIR}_{th\_rc,6mbps}} \cdot d_{tx\_\ell,6mbps} \end{aligned} \tag{17}$$

and the radius of the interference range, when the interference is caused by CTS frames, is

$$\begin{aligned} r_{i(cts)}^+ &= \sqrt[4]{\alpha \cdot \mathrm{SIR}_{th\_rc,6mbps}} \cdot d_{tx\_rc,6mbps} \\ &> \sqrt[4]{\alpha} \cdot d_{tx\_rc,6mbps} = r_r^+ \end{aligned} \tag{18}$$

Therefore, the data frame reception may still be interfered with by the CTS signals.

4) RTS(Strong)-CTS-Data(TPC)-Ack: Another way of dealing with the aggravated interference problem caused by TPC is to transmit the RTS frames at a stronger power level ($\mathcal{P}_{rts^+} = \beta \cdot \mathcal{P}_{nom}$ with $\beta > 1$). Following a similar analysis to that in Section III-D3, it is easy to show that, when $\beta \geqslant ((d/d_{tx\_rc,6mbps}) + \sqrt[4]{\mathrm{SIR}_{th\_rc,6mbps}})^4$, the data frame reception will never be interfered with by any CTS, Data, or Ack frames from neighboring stations but may be interfered with by the RTS signals. The analysis details are omitted due to space limitation. Interested readers please refer to [25].

One key observation from Sections III-D3 and III-D4 is that, the TPC-caused interference problem may be dealt with by either transmitting the CTS frames at $\mathcal{P}_{cts^+} = \alpha \cdot \mathcal{P}_{nom}$ or transmitting the RTS frames at $\mathcal{P}_{rts^+} = \beta \cdot \mathcal{P}_{nom}$ with $\alpha < \beta$, meaning that the former scheme is more energy-efficient. For this reason, we choose the enhanced

RTS-CTS(strong)-Data(TPC)-Ack handshake to accommodate our intelligent TPC mechanism, and in particular, the CTS frames are transmitted at 5 dB higher than, or equivalently, $\alpha = 3.16$ times, the nominal transmit power. Since we let $\mathcal{P}_{nom}$ be 15 dBm, $\mathcal{P}_{cts^+}$ is 20 dBm and conforms to the 23-dBm transmit power limitation.[3] Moreover, as $\mathrm{SIR}_{th\_rc,6mbps}$ is typically less than or equal to 5 dB,[4] so with *RTS-CTS(strong)-Data(TPC)-Ack*, the data frame reception will never be interfered with by any RTS, Data, or Ack frame transmissions from neighboring stations. Although it may still be interfered with by the CTS signals, considering the fact that the CTS frames are normally much shorter than the data frames, such interference is not as severe as that caused by the data signals, which may occur when the conventional four-way handshake is used.

E. Summary

We summarize the interference analysis results as follows.

- Without RTS/CTS support, applying TPC on data transmissions may result in more hidden nodes and aggravate the interference.
- With RTS/CTS support, the "hidden nodes" problem is alleviated and the CCA busy range is completely covered by the NAV set range in 802.11a systems. However, applying TPC on data transmissions may still aggravate the interference due to the enlarged interference range.
- Both *RTS-CTS(strong)-Data(TPC)-Ack* and *RTS(strong)-CTS-Data(TPC)-Ack* schemes are suitable to accommodate intelligent TPC in 802.11a systems, because they not only allow data frames to be transmitted at lower power levels to save energy, but also ameliorate the potentially aggravated interference caused by TPC by transmitting CTS or RTS frames at stronger power levels.
- The enhanced *RTS-CTS(strong)-Data(TPC)-Ack* handshake is more energy efficient than *RTS(strong)-CTS-Data(TPC)-Ack* and, hence, is selected to accommodate our intelligent TPC mechanism.

IV. MiSer

MiSer [10] is our intelligent TPC mechanism for 802.11a/h DCF systems. In order to deal with the "hidden nodes" problem and the TPC-caused interference, MiSer is deployed in the format of *RTS-CTS(strong)-Data(MiSer)-Ack*, which was discussed in Section III-D3.

MiSer is motivated by [28] and is a simple table-driven approach. The basic idea is that the wireless station computes offline a rate–power combination table indexed by the data transmission status and each entry of the table is the optimal rate–power combination $(\langle \mathcal{R}^*, \mathcal{P}_t^* \rangle)$ in the sense of maximizing the energy efficiency $(\mathcal{J})$ under the corresponding data transmission status. The *data transmission status* is characterized by a quintuplet: $(\ell, a, s, \mathrm{SRC}, \mathrm{LRC})$, where ℓ is the data payload length, a is the path loss from the transmitter to the receiver, s is the interference plus noise level observed by the receiver—i.e., the receiver-side wireless channel condition, and (SRC, LRC) are the frame retry counts. The *energy efficiency* $(\mathcal{J})$ is defined as the ratio of the expected delivered data payload $(\mathcal{L})$ to the expected total energy consumption $(\mathcal{E})$. This table is then used at runtime to determine the proper PHY rate and transmit power for each data transmission attempt.

A. Step I: Offline Establishment of the Rate–Power Combination Table

We assume that the transmission error (due to background noise) probabilities of the RTS, CTS, and Ack frames are negligible because of their small frame sizes and robust transmission rates (refer to Section III-C). Then, the table entries of the rate–power combination table are computed as follows. At first, let us consider the general case when

$$0 \leqslant \mathrm{SRC} < dot11ShortRetryLimit \tag{19}$$

and

$$0 \leqslant \mathrm{LRC} < dot11LongRetryLimit. \tag{20}$$

Assume that $\langle \mathcal{R}, \mathcal{P}_t \rangle$ is selected for the data transmission attempt of status $(\ell, a, s, \mathrm{SRC}, \mathrm{LRC})$. Also, assume that the future retransmission attempts, if any, will be made with the most energy-efficient transmission strategies as well. Clearly, the frame delivery is successful only if the RTS transmission succeeds without collision and the data transmission is error-free or results in correctable errors. Otherwise, the station has to re-contend for the medium to retransmit the frame. In particular, if the delivery failure was due to RTS collision, the frame retry counts become (SRC + 1, LRC); if the delivery failure was due to erroneous reception of the data frame, the frame retry counts become (SRC, LRC + 1).

We use $f_{\mathcal{A}}(a'|a)$ to denote the conditional probability density function that, given the current path loss condition of a, the path loss condition becomes a' during the next transmission attempt. Similarly, we use $f_{\mathcal{S}}(s'|s)$ to denote the conditional probability density function that, given the current wireless channel condition of s, the channel condition becomes s' during the next transmission attempt. Notice that these two density functions vary with the time elapsed between two transmission attempts, and different wireless channel variation models can be characterized by different $f_{\mathcal{A}}(a'|a)$ and $f_{\mathcal{S}}(s'|s)$ functions.

Based on the above observations, the expected delivered data payload $(\mathcal{L})$ and the expected total energy consumption $(\mathcal{E})$ can be calculated (recursively) by (21) and (22), respectively, as shown at the bottom of the next page, where $P_{c,rts}$ is the RTS collision probability, $P_{e,data}$ is the data transmission error probability, which is a function of $\mathcal{R}$, $\mathcal{P}_t$, ℓ, a, and s and varies with the wireless channel model [27], and

$$\mathcal{E}_{rts-sifs-cts-sifs} = \mathcal{E}_{rts} + 2 \cdot \mathcal{E}_{sifs} + \mathcal{E}_{cts}. \tag{23}$$

[3]According to the 802.11 standard [26], the maximum transmit power is limited to 200 mW (i.e., 23 dBm) for the middle band of the 5-GHz U-NII band, which is suitable for indoor environments.

[4]The error probability analysis in [27] shows that, when a data frame with 1152-octet payload is transmitted at 6 Mb/s and the receiver-side SIR is larger than 5 dB, the PER of the frame is extremely small and, hence, negligible.

Since an Ack (CTS) timeout is equal to a SIFS time, plus an Ack (CTS) transmission time, and plus a Slot time, we have

$$\begin{cases} \mathcal{E}_{ack\_tout} = \mathcal{E}_{sifs} + \mathcal{E}_{ack} + \mathcal{E}_{slot}, \\ \mathcal{E}_{cts\_tout} = \mathcal{E}_{sifs} + \mathcal{E}_{cts} + \mathcal{E}_{slot}. \end{cases} \tag{24}$$

Here, $\mathcal{E}_{rts}$, $\mathcal{E}_{data}(\cdot)$, $\mathcal{E}_{cts}$, and $\mathcal{E}_{ack}$ represent the energy consumed to transmit an RTS/Data frame, or receive a CTS/Ack frame, respectively. $\overline{\mathcal{E}}_{bkoff}(\cdot)$ and $\overline{\mathcal{E}}_{freeze}$ constitute the total energy consumption during a backoff period, and represent the energy consumption while the backoff counter is decrementing and the energy consumption while the backoff counter is frozen due to the busy medium, respectively. Moreover, $\mathcal{E}_{sifs}$, $\mathcal{E}_{difs}$, and $\mathcal{E}_{slot}$ denote the energy consumptions of a WLAN device being idle for SIFS time, DIFS time, and Slot time, respectively. The details of the energy consumption calculation are omitted due to space limitation. Interested readers please refer to [10] and [25]. The energy efficiency ($\mathcal{J}$) is thus

$$\mathcal{J}(\mathcal{R}, \mathcal{P}_t, \ell, a, s, \text{SRC}, \text{LRC}) = \frac{\mathcal{L}(\mathcal{R}, \mathcal{P}_t, \ell, a, s, \text{SRC}, \text{LRC})}{\mathcal{E}(\mathcal{R}, \mathcal{P}_t, \ell, a, s, \text{SRC}, \text{LRC})}. \tag{25}$$

Since there are only finite choices for the PHY rate and the transmit power, we can calculate $\mathcal{J}$ for each rate–power combination, and the pair that maximizes $\mathcal{J}$ is then the most energy-efficient strategy for the data transmission attempt of status $(\ell, a, s, \text{SRC}, \text{LRC})$:

$$\begin{aligned} &\langle \mathcal{R}^*(\ell, a, s, \text{SRC}, \text{LRC}), \mathcal{P}_t^*(\ell, a, s, \text{SRC}, \text{LRC}) \rangle \\ &\quad = \arg \max_{\langle \mathcal{R}, \mathcal{P}_t \rangle} \mathcal{J}(\mathcal{R}, \mathcal{P}_t, \ell, a, s, \text{SRC}, \text{LRC}). \end{aligned} \tag{26}$$

Now, consider the special case when

$$\text{SRC} = dot11ShortRetryLimit \tag{27}$$

and/or

$$\text{LRC} = dot11LongRetryLimit. \tag{28}$$

Obviously, since at least one of the frame retry limits has been reached, the data frame will be discarded without further transmission attempt. Hence, for any $\langle \mathcal{R}, \mathcal{P}_t \rangle$, we always have

$$\begin{cases} \mathcal{E}(\mathcal{R}, \mathcal{P}_t, \ell, a, s, dot11ShortRetryLimit, \text{LRC}) = 0, \\ \mathcal{L}(\mathcal{R}, \mathcal{P}_t, \ell, a, s, dot11ShortRetryLimit, \text{LRC}) = 0 \end{cases} \tag{29}$$

and

$$\begin{cases} \mathcal{E}(\mathcal{R}, \mathcal{P}_t, \ell, a, s, \text{SRC}, dot11LongRetryLimit) = 0, \\ \mathcal{L}(\mathcal{R}, \mathcal{P}_t, \ell, a, s, \text{SRC}, dot11LongRetryLimit) = 0. \end{cases} \tag{30}$$

Using this special case as the boundary condition, we have fully specified the computation of the rate–power combination table by (21), (22), (25), (26), (29), and (30).

B. Step II: Runtime Execution

Before communication starts, a wireless station computes the optimal rate–power combination for each set of data payload length (ℓ), path loss (a), wireless channel condition (s), and frame retry counts (SRC, LRC). Thus, a rate–power combination table is pre-established and ready for runtime use. At runtime, the wireless station estimates the path loss between itself and the receiver, monitors the wireless channel condition,

---

$$\begin{aligned} \mathcal{L}(\mathcal{R}, \mathcal{P}_t, \ell, a, s, \text{SRC}, \text{LRC}) &= (1 - P_{c,rts}) \cdot [1 - P_{e,data}(\mathcal{R}, \mathcal{P}_t, \ell, a, s)] \cdot \ell + (1 - P_{c,rts}) \cdot P_{e,data}(\mathcal{R}, \mathcal{P}_t, \ell, a, s) \\ &\quad \cdot \int_{-\infty}^{\infty} f_{\mathcal{A}}(a'|a) \int_{-\infty}^{\infty} f_{\mathcal{S}}(s'|s) \mathcal{L}\left(\mathcal{R}^*(\ell, a', s', \text{SRC}, \text{LRC}+1), \mathcal{P}_t^*(\ell, a', s', \text{SRC}, \text{LRC}+1), \ \ell, a', s', \text{SRC}, \text{LRC}+1\right) ds' da' \\ &\quad + P_{c,rts} \cdot \int_{-\infty}^{\infty} f_{\mathcal{A}}(a'|a) \int_{-\infty}^{\infty} f_{\mathcal{S}}(s'|s) \mathcal{L}\left(\mathcal{R}^*(\ell, a', s', \text{SRC}+1, \text{LRC}), \ \mathcal{P}_t^*(\ell, a', s', \text{SRC}+1, \text{LRC}), \ell, a', s', \text{SRC}+1, \text{LRC}\right) ds' da'. \end{aligned} \tag{21}$$

$$\begin{aligned} \mathcal{E}(\mathcal{R}, \mathcal{P}_t, \ell, a, s, \text{SRC}, \text{LRC}) &= \overline{\mathcal{E}}_{bkoff}(\text{SRC}, \text{LRC}) + \overline{\mathcal{E}}_{freeze} \\ &\quad + (1 - P_{c,rts}) \cdot [1 - P_{e,data}(\mathcal{R}, \mathcal{P}_t, \ell, a, s)] \cdot [\mathcal{E}_{rts-sifs-cts-sifs} + \mathcal{E}_{data}(\mathcal{R}, \mathcal{P}_t, \ell) + \mathcal{E}_{sifs} + \mathcal{E}_{ack} + \mathcal{E}_{difs}] \\ &\quad + (1 - P_{c,rts}) \cdot P_{e,data}(\mathcal{R}, \mathcal{P}_t, \ell, a, s) \cdot [\mathcal{E}_{rts-sifs-cts-sifs} + \mathcal{E}_{data}(\mathcal{R}, \mathcal{P}_t, \ell) + \mathcal{E}_{ack\_tout} \\ &\qquad + \int_{-\infty}^{\infty} f_{\mathcal{A}}(a'|a) \int_{-\infty}^{\infty} f_{\mathcal{S}}(s'|s) \mathcal{E}\left(\mathcal{R}^*(\ell, a', s', \text{SRC}, \text{LRC}+1), \ \mathcal{P}_t^*(\ell, a', s', \text{SRC}, \text{LRC}+1), \ \ell, a', s', \text{SRC}, \text{LRC}+1\right) ds' da'] \\ &\quad + P_{c,rts} \cdot [\mathcal{E}_{rts} + \mathcal{E}_{cts\_tout} \\ &\qquad + \int_{-\infty}^{\infty} f_{\mathcal{A}}(a'|a) \int_{-\infty}^{\infty} f_{\mathcal{S}}(s'|s) \mathcal{E}\left(\mathcal{R}^*(\ell, a', s', \text{SRC}+1, \text{LRC}), \ \mathcal{P}_t^*(\ell, a', s', \text{SRC}+1, \text{LRC}), \ \ell, a', s', \text{SRC}+1, \text{LRC}\right) ds' da']. \end{aligned} \tag{22}$$

and then selects the most energy-efficient rate–power combination for the current data transmission attempt by a simple table lookup. Note that the rate–power selection shall be made before the RTS frame is transmitted, so that the Duration/ID information carried in the RTS frame can be properly set according to the PHY rate selection.

Since MiSer shifts the computation burden offline, its runtime execution is simplified significantly. As a result, embedding MiSer at the MAC layer has little effects on the performance of higher-layer applications, which is a desirable feature for any MAC-layer enhancement.

C. Implementation Issues

1) Table Establishment: As described in Section IV-A, in order to establish the rate–power combination table, a wireless station needs the following information:

- the number of contending stations and the RTS collision probability $(P_{c,rts})$;
- wireless channel models that determine the error performances of the PHY rates $(P_{e,data})$ and the conditional probability density functions $f_{\mathcal{A}}(a'|a)$ and $f_{\mathcal{S}}(s'|s)$.

There have been many papers dealing with the problems of estimating the number of contending stations and the collision probability [29]–[32] or building accurate wireless channel models [33]–[36], which are not the focus of this paper. Our contribution is the development of MiSer as a simple and effective TPC mechanism by assuming that the wireless station either has the required knowledge *a priori* or can estimate them.

2) Path Loss Estimation: At runtime, in order to look up the pre-established rate–power combination table to determine the best transmission strategy for each data frame, a wireless station has to estimate the path loss between itself and the receiver. We have developed a simple path loss estimation scheme, based on the 802.11h standard [15], as a possible solution.

The 802.11h standard is an extension to the 802.11 MAC and the 802.11a PHY, and one of the key improvements in 802.11h is to enable a wireless station to report its transmit power information in the newly defined TPC Report element, which includes a Transmit Power field and a Link Margin field. The Transmit Power field simply contains the transmit power (in dBm) used to transmit the frame containing the TPC Report element, while the Link Margin field contains the link margin (in dB) calculated as the ratio of the received signal strength to the minimum desired by the station.

As specified in the 802.11h standard, the AP in an infrastructure network or a wireless station in an ad hoc network will autonomously include a TPC Report element with the Link Margin field set to zero and containing its transmit power information in the Transmit Power field in any Beacon or Probe Response frame it transmits. A wireless station keeps track of the path loss to the AP, if within an infrastructure network,[5] or the path loss to each neighboring station, if within an ad hoc network, and whenever it receives a Beacon or Probe Response frame, it updates the corresponding path loss value. That is, with the knowledge of the received signal strength (in dBm) via RSSI (receive signal strength indicator) as well as the transmit power (in dBm) via the TPC Report element found in the frame, the wireless station can calculate the path loss (in dB) from the sending station to itself by performing a simple subtraction. Note that RSSI is one of the RXVECTOR parameters, which is measured and passed to the MAC by the PHY and indicates the energy observed at the antenna used to receive the current frame. Basically, the path loss value(s) maintained in this manner can be used by the wireless station to determine its best transmission strategy.

This path loss estimation scheme is reasonable since with 802.11 systems, the same frequency channel is used for all transmissions in a time-division duplex manner, and hence, the channel characteristics in terms of path loss for both directions are likely to be similar. Moreover, since the Beacon frames are transmitted periodically and frequently, a wireless station is able to update the path loss value(s) in a timely manner.

3) Optimality of MiSer: As shown in Section IV-A, MiSer is designed to be the optimal low-energy transmission strategy for 802.11a/h. However, its optimality is based on the assumption of perfect knowledge on the number of contending stations, the RTS collision probability, the wireless channel models, and accurate estimation of the path loss. Therefore, MiSer can be viewed as a benchmark study on the energy-efficient transmission in 802.11a/h systems, which answers an important question: *what is the upper bound on energy conservation by applying TPC on data transmissions?* In reality, with less accurate knowledge on the required information, MiSer will be inevitably less effective.

V. Performance Evaluation

We evaluate the performance of MiSer using the ns-2 simulator [37] after enhancing the original 802.11 DCF module of ns-2 to support the 802.11a/h PHY, PHY rate adaptation, and TPC (transmit power control).

A. Simulation Setup

In the simulation, we use 15 dBm as the nominal transmit power, and a TPC-enabled 802.11a/h device is allowed to choose any one of the 31 power levels (from -15 dBm to 15 dBm with 1-dBm gaps) to transmit a data frame. As well, we simulate the energy consumption behavior of the 802.11a/h devices according to the energy consumption model that we proposed in [10]. We assume an additive white gaussian noise (AWGN) wireless channel model and the background noise level is set to -93 dBm. Moreover, we use a log-distance path loss model with path loss exponent of four to simulate the indoor office environment, and set the carrier sensing threshold to -91 dBm, meaning that, when the distance between two stations is larger than 28.6 meters, the resulting path loss is larger than 106 $(= 15 + 91)$ dB and these two stations are hidden to each other.

In the first part of the simulation, we compare MiSer against four testing schemes with RTS/CTS support: the PHY rate adaptation scheme without TPC (RA), and three single-rate TPC schemes using PHY rate 6 Mb/s (Tpc/R6), 24 Mb/s (Tpc/R24), and 54 Mb/s (Tpc/R54), respectively. The comparison metrics are the aggregate goodput (in Mb/s) and the delivered data per unit of energy consumption (in Mb/Joule), which is calculated

[5]In an infrastructure DCF system, if a wireless station wants to communicate with another station, the frames must be first sent to the AP, and then from the AP to the destination [26]. Therefore, a wireless station only needs to keep track of the path loss between itself and the AP.

as the ratio of the total amount of data delivered by the transmitter stations over their total energy consumption. Note that the larger this value, the more energy-efficient a scheme becomes. We conduct the simulation with various network topologies, various data payload lengths, and various numbers of contending stations.

In the second part of the simulation, we compare MiSer against two schemes without RTS/CTS support: the rate–power adaptation scheme (DA-I) and the rate adaptation only scheme (DA-II). In addition to the aggregate goodput and the delivered data per unit of energy consumption, we also compare the frame collision probability for the testing schemes.

Each simulation run lasts 120 seconds in an 802.11a/h DCF system with multiple transmitter stations contending for the shared wireless medium. Each station transmits in a greedy mode, i.e., its data queue is never empty, and all the data frames are transmitted without fragmentation. All stations are static. Unless specified otherwise, the number of contending stations is eight and the frame size is 1500 octets.

Note that MiSer's rate–power combination table is obtained by following the recursive steps specified in Section IV-A, while RA's rate adaptation table or Tpc/Rx's ($x = 6$, 24, or 54) power adaptation table are computed in the same way as MiSer's rate–power combination table, except fixing the transmit power to 15 dBm or the transmission rate to x Mb/s, respectively. Moreover, in order to have a fair evaluation on the effects of RTS/CTS support, we simply let DA-I and DA-II use MiSer's rate–power combination table to determine their transmission strategies.

B. MiSer Versus Schemes With RTS/CTS Support

1) Star Topologies With Various Radii: We first compare the testing schemes in star-topology networks, where eight transmitter stations are evenly spaced on a circle around one common receiver with the radius of r $(1 \leqslant r \leqslant 28)$ meters. Although ideal star-topology networks are rarely found in the real world, the simulation results plotted in Fig. 9 help us understand better how TPC adapts to the path loss variation and why MiSer is superior to other simulated transmission strategies, thanks to the symmetric station deployment of star-topology networks, and hence, are valuable.

In general, as r increases, both the aggregate goodput and the delivered data per Joule decrease for all testing schemes. This is because more robust transmission strategies (i.e., lower rate and/or higher power) are used to deal with the increasing number of hidden terminals and the larger path loss between the transmitter and the receiver. However, different schemes show different decreasing curves determined by their respective design philosophies, which are discussed next. In order to have a better understanding of the figure, we list, in Table I, the rate–power selections by each testing scheme, when $r = 5$, 9, 12, and 28, respectively.

RA achieves the highest aggregate goodput because its constant use of the strong 15 dBm transmit power allows it to choose the highest possible rate to transmit a data frame. On the other hand, since RA does not support TPC, so even within a small network, it still has to transmit a frame using a higher power than necessary over a short distance, hence consuming more energy. For example, as shown in Table I, when $r = 5$, MiSer selects

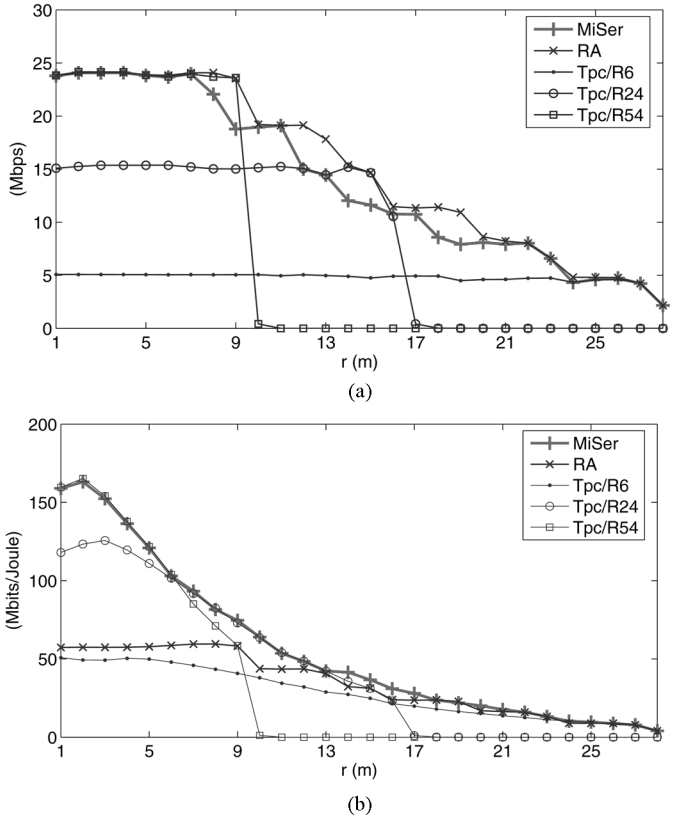

Fig. 9. Comparison for star-topology networks (various radii). (a) Aggregate goodput. (b) Delivered data per unit of energy consumption.

TABLE I
EXAMPLE RATE–POWER SELECTIONS $((\mathrm{SRC}, \mathrm{LRC}) = (0, 0))$

r (m)	rate-power selection (<Mbps, dBm>)			
	5	9	12	28
MiSer	<54, 5>	<36, 9>	<24, 11>	<6, 15>
RA	<54, 15>	<54, 15>	<36, 15>	<6, 15>
Tpc/R6	<6, -13>	<6, -3>	<6, 2>	<6, 15>
Tpc/R24	<24, -3>	<24, 6>	<24, 11>	<24, 15>
Tpc/R54	<54, 5>	<54, 15>	<54, 15>	<54, 15>

the same 54 Mb/s rate as RA, but a much lower transmit power level at 5 dBm. As a result, RA yields much lower delivered data per Joule than MiSer when r is small.

Tpc/R6 transmits all the data frames at the lowest 6 Mb/s, and hence, results in the lowest aggregate goodput when r is small. As r increases, Tpc/R6 adjusts its transmit power adaptively such that the receiver-side SINR is maintained at a relatively stable level. For example, as shown in Table I, when r increases from 5 to 9, 12, and 28, Tpc/R6 increases its transmit power from -13 dBm to -3 dBm, 2 dBm, and 15 dBm, respectively. Therefore, combined with rate 6 Mb/s' strong error-correcting capability, Tpc/R6 shows an almost flat aggregate-goodput curve but a decreasing curve for the delivered data per Joule until $r = 28$, when the most conservative combination of 6 Mb/s and 15 dBm is still not robust enough to combat the resulting high path loss.

Tpc/R54 transmits all the data frames at the highest 54 Mb/s. Similar to Tpc/R6, it also has a flat aggregate-goodput curve when r is small. However, due to rate 54 Mb/s' poor error-correcting capability, the aggregate-goodput curve starts dipping at

a much smaller r value of 10. Actually, when $r > 10$, all the transmission attempts fail and the aggregate goodput drops to zero. Similar observations can be made for Tpc/R24 as well, which is a compromise between Tpc/R6 and Tpc/R54.

So we can see that, because of fixing the transmission rate, a single-rate TPC scheme either suffers a reduced transmission range (e.g., Tpc/R24 and Tpc/R54) or has to keep a low transmission rate (e.g., Tpc/R6).

MiSer achieves the highest delivered data per Joule because of its adaptive use of 1) the energy-efficient combination of high rate and low power when r is small, and 2) the robust combination of low rate and high power when r is large. The key idea is to select the optimal rate–power combination, rather than the PHY rate or the transmit power alone, to minimize the energy consumption. Therefore, under certain path loss conditions (e.g., $r = 9$ in Table I), MiSer may choose a lower rate than RA but with weaker transmit power. As a result, MiSer shows an aggregate goodput curve slightly lower than that of RA. Note that MiSer has the same transmission range as RA and Tpc/R6, since a transmitter station that supports MiSer can always lower the PHY rate and/or increase the transmit power, whenever necessary, to communicate with a far-away receiver station. Another observation in Fig. 9 is that, when 6 Mb/s (or 24 Mb/s, 54 Mb/s) or 15 dBm is part of the optimal rate–power selections, MiSer is indeed equivalent to Tpc/R6 (or Tpc/R24, Tpc/R54) or RA, which is evidenced by the partial overlapping in both their aggregate-goodput curves and their curves for the delivered data per Joule.

2) Random Topologies With 50 Different Scenarios: We also evaluate and compare the performances of the testing schemes in randomly generated network topologies: the eight transmitter stations and their (different) respective receivers are randomly placed within a 40 m $\times$ 40 m flat area. We simulate 50 different scenarios and results are plotted in Fig. 10.

We have three observations. First, MiSer and RA are significantly better than single-rate TPC schemes, in terms of both the aggregate goodput and the delivered data per Joule, in each simulated random topology. This is because the inevitable low transmission rate or reduced transmission range of a single-rate TPC scheme, where the latter may cause more potential transmission failures, results in poor aggregate-goodput and energy-efficiency performances. On the other hand, both MiSer and RA are able to perform PHY rate adaptation, which adjusts the transmission rate dynamically to the path loss variation.

Second, MiSer achieves comparable aggregate goodput with RA while delivering about 15% (on average) more data per unit of energy consumption than RA. Actually, the energy saving by MiSer over RA could be more significant if the network size is smaller. This is because, in a smaller network, the transmitter and the receiver are, on average, closer to each other, which corresponds to a smaller path loss value. As a result, MiSer may choose a much lower transmit power (than 15 dBm) to transmit a frame, thus saving more energy. On the other hand, when the network size gets larger, the energy-efficiency performances of MiSer and RA become comparable.

Third, Tpc/R6 produces near-constant aggregate goodput regardless of the network topology, which is consistent with a similar observation in Fig. 9. Besides, unlike in the small star-topology networks, where Tpc/R54 has the best energy performance, Tpc/R54 has the lowest delivered data per Joule in every scenario due to the arbitrary station locations in random-topology networks. Particularly, in two of the 50 simulated scenarios, Tpc/R54 results in almost zero aggregate goodput.

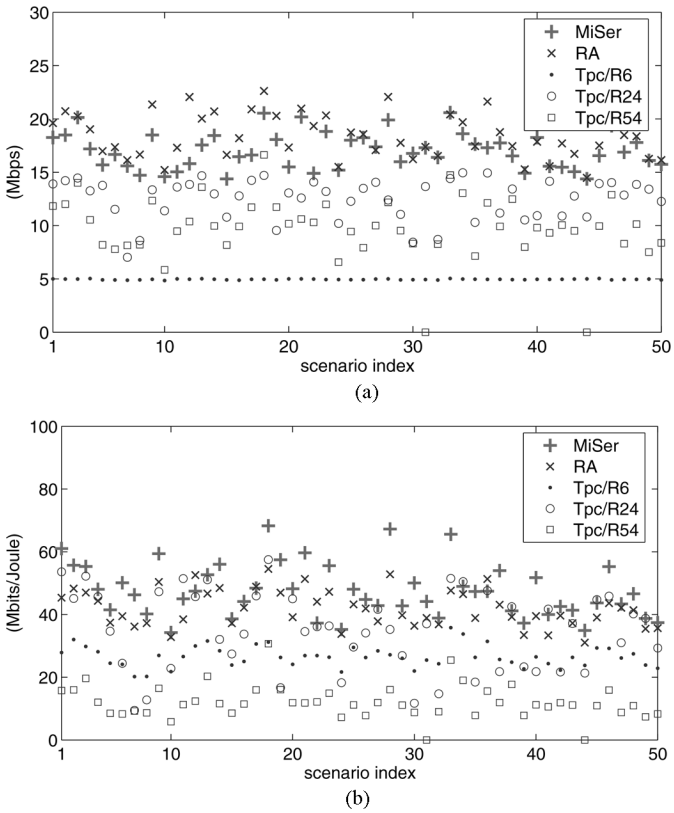

Fig. 10. Comparison for random-topology networks (50 different scenarios). (a) Aggregate goodput. (b) Delivered data per unit of energy consumption.

3) Random Topologies With Various Data Payloads: Fig. 11 shows the simulation results for random-topology networks with various data payloads. The simulated data payload lengths are 32, 64, 128, 256, 512, 1024, and 1500 octets. Each point in the figure is plotted with 90% confidence interval.

Since RTS/CTS frames are always transmitted at 6 Mb/s, the RTS/CTS overhead per data transmission attempt is independent of the payload length. Moreover, there are a number of fixed per-frame overheads such as the MAC header, the frame check sequence (FCS), the PLCP preamble/header, and so on. Hence, both the aggregate goodput and the delivered data per Joule increase with the data payload length for all testing schemes. As expected, MiSer has the best energy-efficiency performance, and the gap between MiSer and RA becomes bigger as the data payload length increases. This is because, with the same PHY rate, a larger data payload results in a longer transmission time, during which MiSer may use low transmit power to save more energy. Moreover, RA outperforms single-rate TPC schemes in terms of both goodput and energy consumption due to PHY rate adaptation.

4) Random Topologies With Various Numbers of Contending Stations: Fig. 12 shows the simulation results for

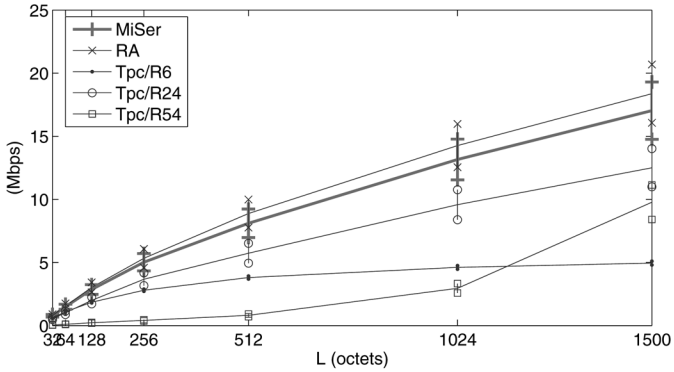

(a)

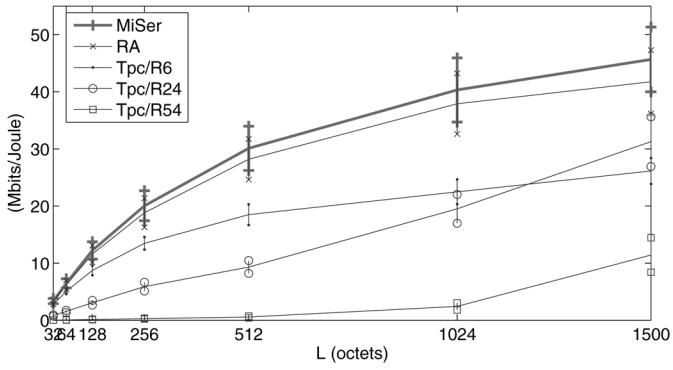

(b)

Fig. 11. Comparison for various data payloads. (a) Aggregate goodput. (b) Delivered data per unit of energy consumption.

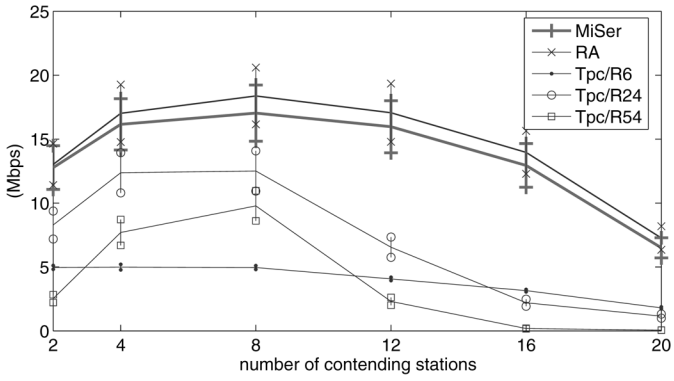

(a)

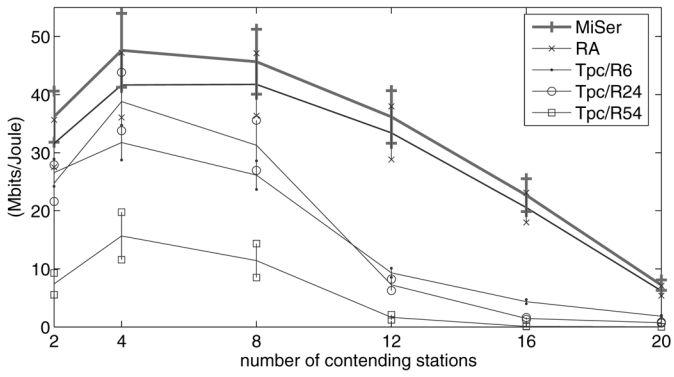

(b)

Fig. 12. Comparison for various numbers of contending stations. (a) Aggregate goodput. (b) Delivered data per unit of energy consumption.

TABLE II
RATE-POWER SELECTIONS BY THREE TESTING SCHEMES AND RESULTANT HIDDEN NODE RATIOS IN STAR-TOPOLOGY NETWORKS

r (m)	rate-power selection (<Mbps, dBm>) and δ					
	MiSer		DA-I		DA-II	
9	<36, 9>	0	<36, 9>	0	<36, 15>	0
15	<18, 12>	1/7	<18, 12>	3/7	<18, 15>	1/7
22	<12, 15>	5/7	<12, 15>	5/7	<12, 15>	5/7

random-topology networks with various numbers of contending stations: 2, 4, 8, 12, 16, and 20. Each point in the figure is plotted with 90% confidence interval.

Although MiSer has the best energy-efficiency performance under all simulated scenarios, as the number of contending stations increases, the performance gain of MiSer over other schemes becomes less significant. This is because, as the network becomes more crowded, it is more likely that the frame transmission attempts will collide with each other. As a result, energy spent on collision resolution becomes the dominant part of the total energy consumption. As shown in the figure, without an effective collision resolution scheme, the benefit of applying TPC on data transmissions is limited when the number of contending stations gets large.

C. MiSer Versus Schemes Without RTS/CTS Support

We now compare the performance of MiSer against schemes without RTS/CTS support. We introduce a new measure called the *hidden node ratio* (δ) of the network, which is defined as the ratio of the number of hidden nodes (average over all transmitter stations) to the total number of contending stations. Clearly, the δ value varies with the network topology, the network size, and the transmit power. We evaluate the performances of the testing schemes in star-topology networks of different sizes, and Table II lists the r values and the corresponding hidden node ratios when different testing schemes are used. We also compare the testing schemes in randomly generated network topologies that were used in Section V-B2. The comparison results are plotted in Fig. 13.

We have two observations. First, when there are no hidden nodes in the network ($r = 9$), all three schemes result in similar frame collision probabilities, and MiSer yields a lower aggregate goodput than DA-I/II due to the additional RTS/CTS overhead. However, since MiSer is able to select a lower power level (at 9 dBm) for its data transmissions, it shows comparable energy-efficiency performance with DA-II that always transmits at 15 dBm.

Second, when there are hidden nodes in the network ($r = 15$ or 22, or random), the performances of all three schemes degrade. With a larger hidden node ratio, more stations are hidden to each other in the network and the frame collision probability increases, thus the performance degrades even more. MiSer is less affected by the presence of hidden nodes than DA-I/II because, by exchanging RTS/CTS frames to reserve the wireless channel before actual data transmissions, collisions can only occur to the RTS frames that are much shorter than the data frames. For this reason, MiSer outperforms DA-I/II significantly in terms of both the aggregate goodput and the delivered data per unit of energy consumption.

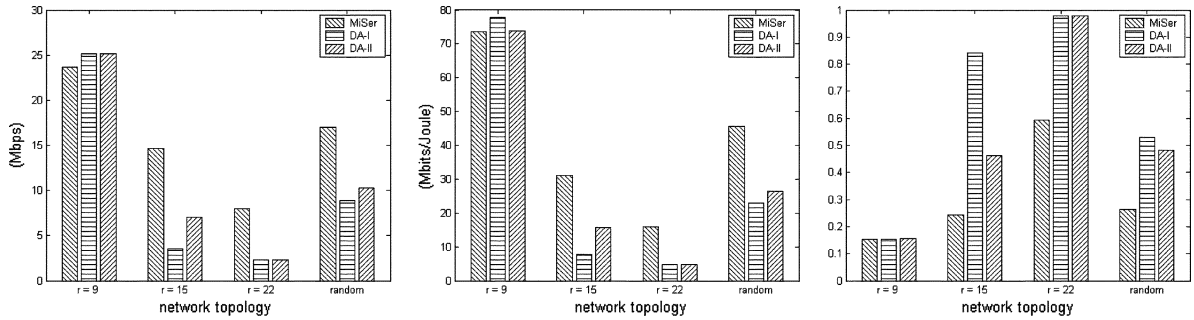

Fig. 13. Comparison of MiSer against schemes without RTS/CTS support. (a) Aggregate goodput. (b) Delivered data per unit of energy consumption. (c) Frame collision probability.

As discussed in Section III-B, one potential problem of applying TPC on data transmissions without RTS/CTS support is that it might result in more hidden nodes. We observe such scenario in the simulated network of $r = 15$. In this case, DA-I selects the rate–power combination of 18 Mb/s and 12 dBm for the data transmissions, while MiSer and DA-II contend for the wireless channel by transmitting its RTS or data frames at the 15 dBm power level. As a result, when DA-I is used, the hidden node ratio of the network becomes 3/7 instead of 1/7. The fact explained above is supported by the drastically higher frame collision probability for DA-I when $r = 15$.

D. Summary

Based on the observations from the simulation results, we summarize MiSer as follows:

- In order to save energy by applying TPC on data transmissions, RTS/CTS support is essential to alleviate the "hidden nodes" problem.
- MiSer is deployed as *RTS-CTS(strong)-Data(MiSer)-Ack*.
- When the number of contending stations is reasonably small, MiSer is significantly better than any other scheme (with RTS/CTS support) that simply adapts the PHY rate or adjusts the transmit power.
- Without an effective collision resolution scheme, the performance gains of intelligent TPC schemes, including MiSer, become less significant when the number of contending stations gets large.
- PHY rate adaptation is very effective in saving energy and plays an important role in MiSer.
- Applying MiSer does not affect the transmission range.
- MiSer is most suitable for data communications with large data payloads.

VI. Conclusion

In this paper, we investigate the problem of minimizing the communication energy consumption in 802.11a/h systems. Based on the analysis of the relationship among different radio ranges and TPC's effects on the interference in 802.11a systems, we propose MiSer, a novel intelligent TPC mechanism, as an optimal solution. The key idea is to combine TPC with PHY rate adaptation, so that the most energy-efficient rate–power combination can be adaptively selected for each data transmission attempt. It establishes an optimal rate–power combination table before the communication starts, which shifts the computation burden offline, and hence, simplifies the runtime execution (to simple table lookups) significantly. MiSer is deployed in the format of *RTS-CTS(strong)-Data(MiSer)-Ack* to alleviate the "hidden nodes" problem and to ameliorate the TPC-caused interference in the network.

Our in-depth simulation shows that MiSer is significantly better than the schemes without RTS/CTS support in the presence of hidden nodes, which are often found in the real networks. Moreover, compared with other schemes with RTS/CTS support, when the number of contending stations in the network is reasonably small, MiSer clearly outperforms the single-rate TPC schemes and is much more energy-efficient than the PHY rate adaptation scheme without TPC.

References

[1] M. Stemm, P. Gauthier, D. Harada, and R. H. Katz, "Reducing power consumption of network interfaces in hand-held devices," in *Proc. 3rd Int. Workshop on Mobile Multimedia Communications*, Princeton, NJ, Sep. 1996.

[2] T. Simunic, L. Benini, P. Glynn, and G. D. Micheli, "Dynamic power management for portable systems," in *Proc. ACM MobiCom'00*, Boston, MA, Aug. 2000, pp. 11–19.

[3] E.-S. Jung and N. H. Vaidya, "An energy efficient MAC protocol for wireless LANs," in *Proc. IEEE INFOCOM'02*, New York, Jun. 2002, vol. 3, pp. 1756–1764.

[4] R. Krashinsky and H. Balakrishnan, "Minimizing energy for wireless web access with bounded slowdown," in *Proc. ACM MobiCom'02*, Atlanta, GA, Sep. 2002, pp. 119–130.

[5] M. Anand, E. B. Nightingale, and J. Flinn, "Self-tuning wireless network power management," in *Proc. ACM MobiCom'03*, San Diego, CA, Sep. 2003, pp. 176–189.

[6] J. Gomez, A. T. Campbell, M. Naghshineh, and C. Bisdikian, "Conserving transmission power in wireless ad hoc networks," in *Proc. IEEE ICNP'01*, Nov. 2001, pp. 24–34.

[7] S. Agarwal, S. V. Krishnamurthy, R. K. Katz, and S. K. Dao, "Distributed power control in ad-hoc wireless networks," in *Proc. IEEE PIMRC'01*, 2001, pp. 59–66.

[8] E.-S. Jung and N. H. Vaidya, "A power control MAC protocol for ad hoc networks," in *Proc. ACM MobiCom'02*, Atlanta, GA, Sep. 2002, pp. 36–47.

[9] J.-P. Ebert and A. Wolisz, "Combined tuning of RF power and medium access control for WLANs," *Mobile Networks Applicat.*, vol. 5, no. 6, pp. 417–426, Sep. 2001.

[10] D. Qiao, S. Choi, A. Jain, and K. G. Shin, "MiSer: An optimal low-energy transmission strategy for IEEE 802.11a/h," in *Proc. ACM MobiCom'03*, San Diego, CA, Sep. 2003, pp. 161–175.

[11] *Part 11: Wireless LAN Medium Access Control (MAC) and Physical Layer (PHY) Specifications*, IEEE 802.11, Aug. 1999.

[12] *Part 11: Wireless LAN Medium Access Control (MAC) and Physical Layer (PHY) Specifications: High-Speed Physical Layer Extension in the 2.4 GHz Band*, IEEE 802.11b, Sep. 1999, Supplement to IEEE 802.11 Standard.

[13] *Part 11: Wireless LAN Medium Access Control (MAC) and Physical Layer (PHY) Specifications: Further Higher Data Rate Extension in the 2.4 GHz Band*, IEEE 802.11g, Jun. 2003, Supplement to IEEE 802.11 Standard.
[14] *Part 11: Wireless LAN Medium Access Control (MAC) and Physical Layer (PHY) Specifications: High-Speed Physical Layer in the 5 GHz Band*, IEEE 802.11a, Sep. 1999, Supplement to IEEE 802.11 Standard.
[15] *Part 11: Wireless LAN Medium Access Control (MAC) and Physical Layer (PHY) Specifications: Spectrum and Transmit Power Management Extensions in the 5 GHz Band in Europe*, IEEE 802.11h, Oct. 2003, Supplement to IEEE 802.11 Standard-1999 Edition.
[16] S. D. Gray and V. Vadde, *Throughput and Loss Packet Performance of DCF With Variable Transmit Power* , IEEE 802.11-01/227, May 2001.
[17] M. Pursley, H. Russell, and J. Wysocarski, "Energy-efficient transmission and routing protocols for wireless multiple-hop networks and spread-spectrum radios," in *Proc. EuroComm'00*, 2000, pp. 1–5.
[18] M. Pursley, H. Russell, and J. Wysocarski, "Energy-efficient routing in frequency-hop networks with adaptive transmission," in *Proc. IEEE MILCOM'99*, Nov. 1999.
[19] D. Qiao, S. Choi, A. Jain, and K. G. Shin, "Adaptive transmit power control in IEEE 802.11a wireless LANs," in *Proc. IEEE VTC'03-Spring*, Jeju, Korea, Apr. 2003.
[20] A. E. Gamal, C. Nair, B. Prabhakar, E. U. Biyikoglu, and S. Zahedi, "Energy-efficient scheduling of packet transmissions over wireless networks," in *Proc. IEEE INFOCOM'02*, New York, Jun. 2002, vol. 3, pp. 1773–1782.
[21] B. Prabhakar, E. U. Biyikoglu, and A. E. Gamal, "Energy-efficient transmission over a wireless link via lazy packet scheduling," in *Proc. IEEE INFOCOM'01*, Anchorage, AK, Apr. 2001, vol. 1, pp. 386–394.
[22] K. Xu, M. Gerla, and S. Bae, "How effective is the IEEE 802.11 RTS/CTS handshake in ad hoc network," in *Proc. IEEE GlobeCom'02*, Taipei, Taiwan, Nov. 2002.
[23] Netgear WAG511 802.11a/b/g Dual Band Wireless PC Card Data Sheet. Netgear Inc., 2004.
[24] T. S. Rappaport, *Wireless Communications: Principle and Practice*. Englewood Cliffs, NJ: Prentice-Hall, 1996.
[25] D. Qiao, S. Choi, and K. G. Shin, "Interference analysis and transmit power control in IEEE 802.11a/h wireless LANs," Iowa State Univ., Ames, IA, Tech. Rep., Jan. 2007.
[26] B. O'Hara and A. Petrick, *The IEEE 802.11 Handbook: A Designer's Companion*. New York: Standards Information Network, IEEE Press, 1999.
[27] D. Qiao and S. Choi, "Goodput enhancement of IEEE 802.11a wireless LAN via link adaptation," in *Proc. IEEE ICC'01*, Helsinki, Finland, Jun. 2001.
[28] M. Elaoud and P. Ramanathan, "Adaptive use of error-correcting codes for real-time communication in wireless networks," in *Proc. IEEE INFOCOM'98*, San Francisco, CA, Mar. 1998, vol. 2, pp. 548–555.
[29] G. Bianchi and I. Tinnirello, "Kalman Filter estimation of the number of competing terminals in an IEEE 802.11 network," in *Proc. IEEE INFOCOM'03*, San Francisco, CA, Apr. 2003.
[30] D. Zheng and J. Zhang, "A particle filtering approach to the estimation of competing stations in IEEE 802.11 WLANs," in *Proc. IEEE Globecom'05*, St. Louis, MO, Nov. 2005.
[31] G. Bianchi, L. Fratta, and M. Oliveri, "Performance evaluation and enhancement of the CSMA/CA MAC protocol for 802.11 wireless LANs," in *Proc. IEEE PIMRC*, Taipei, Taiwan, Oct. 1996, pp. 392–396.
[32] F. Cali, M. Conti, and E. Gregori, "Dynamic tuning of the IEEE 802.11 protocol to achieve a theoretical throughput limit," *IEEE/ACM Trans. Networking*, vol. 8, no. 6, pp. 785–799, Dec. 2000.
[33] P. Bergamo, D. Maniezzo, A. Giovanardi, G. Mazzini, and M. Zorzi, "An improved Markov chain description for fading processes," in *Proc. IEEE ICC'02*, New York, Apr. 2002, vol. 3, pp. 1347–1351.
[34] J.-P. Ebert and A. Willig, "A Gilbert-Elliot bit error model and the efficient use in packet level simulation," Technical Univ. Berlin, Telecommunication Networks Group, Berlin, Germany, TKN Tech. Rep. TKN-99-002, Mar. 1999.
[35] H. Wang and P. Chang, "On verifying the first-order Markovian assumption for a Rayleigh fading channel model," *IEEE Trans. Vehicular Technol.*, vol. 45, no. 2, pp. 353–357, May 1996.
[36] M. Zorzi, R. R. Rao, and L. B. Milstein, "Error statistics in data transmission over fading channels," *IEEE Trans. Commun.*, vol. 46, no. 11, pp. 1468–1477, Nov. 1998.
[37] The Network Simulator – ns-2. USC/ISI. [Online]. Available: http://www.isi.edu/nsnam/ns/

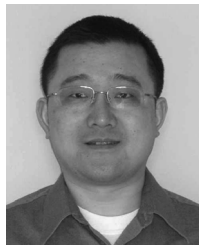

Daji Qiao (S'97–M'04) received the Ph.D. degree in electrical engineering–systems from The University of Michigan, Ann Arbor, in February 2004.

He is an Assistant Professor in the Department of Electrical and Computer Engineering, Iowa State University, Ames. His current research interests include modeling, analysis and protocol/algorithm design for various types of wireless/mobile networks, including IEEE 802.11 wireless LANs, mesh networks, and sensor networks.

Dr. Qiao is a member of the IEEE and the Association for Computing Machinery (ACM).

Sunghyun Choi (S'96–M'00–SM'05) received the B.S. (*summa cum laude*) and M.S. degrees from the Korea Advanced Institute of Science and Technology (KAIST), Daejeon, Korea, in 1992 and 1994, respectively, and the Ph.D. degree from The University of Michigan, Ann Arbor, in September 1999.

He is an Associate Professor in the School of Electrical Engineering, Seoul National University (SNU), Seoul, Korea. Before joining SNU in September 2002, he was with Philips Research USA, Briarcliff Manor, NY, as a Senior Member Research Staff and a project leader for three years. His current research interests are in the area of wireless/mobile networks. He has authored or co-authored over 90 technical papers and book chapters. He holds eight U.S. patents, five European patents, and one Korean patent, and has many patents pending.

Dr. Choi served as a Technical Program Co-Chair of IEEE WoWMoM 2007 and IEEE/Create-Net COMSWARE 2007. He was a Co-Chair of Cross-Layer Designs and Protocols Symposium in IEEE IWCMC 2006, the Workshop Co-Chair of WILLOPAN 2006, the General Chair of ACM WMASH 2005, and a Technical Program Co-Chair for ACM WMASH 2004. He is currently serving and has served on program and organization committees of numerous leading wireless and networking conferences. He is also an area editor of ACM SIGMOBILE *Mobile Computing and Communications Review* (MC2R) and an editor of the *Journal of Communications and Networks* (JCN). He is serving and has served as a guest editor for IEEE JOURNAL ON SELECTED AREAS IN COMMUNICATIONS (JSAC), *IEEE Wireless Communications*, *Wireless Personal Communications*, and *Wireless Communications and Mobile Computing* (WCMC). Since 2000, he has been an active participant and contributor of IEEE 802.11 WLAN Working Group. He is a senior member of the IEEE and a member of the Association for Computing Machinery (ACM), Korean Institute of Communication Sciences (KICS), the Institute of Electronics Engineers of Korea (IEEK), and the Korea Information Science Society (KISS).

Kang G. Shin (S'75–M'78–SM'83–F'92) is the Kevin and Nancy O'Connor Professor of Computer Science and Founding Director of the Real-Time Computing Laboratory in the Department of Electrical Engineering and Computer Science, The University of Michigan, Ann Arbor. His current research focuses on QoS-sensitive networking and computing as well as on embedded real-time OS, middleware and applications, all with emphasis on timeliness and dependability. He has supervised the completion of 56 Ph.D. theses, and authored or co-authored more than 650 technical papers (more than 230 of which are in archival journals) and numerous book chapters in the areas of distributed real-time computing and control, computer networking, fault-tolerant computing, and intelligent manufacturing. He has co-authored (jointly with C. M. Krishna) the textbook *Real-Time Systems* (McGraw-Hill, 1997).

Dr. Shin has received many best paper awards, including the IEEE Communications Society William R. Bennett Prize Paper Award in 2003 and an Outstanding IEEE TRANSACTIONS ON AUTOMATIC CONTROL Paper Award in 1987. He has also received several institutional awards, including the Distinguished Faculty Achievement Award in 2001 and the Stephen Attwood Award in 2004 from The University of Michigan, a Distinguished Alumni Award of the College of Engineering, Seoul National University, in 2002, the 2003 IEEE RTC Technical Achievement Award, and the 2006 Ho-Am Prize in Engineering. He is a Fellow of IEEE and the Association for Computing Machinery (ACM), and a member of the Korean Academy of Engineering.